

An Experiment to Measure the Energy Spectrum of Cosmic Ray  
Antiprotons from 100 to 1000 MeV

M.H. Salamon, P.B. Price, S.W. Barwick, and D.M. Lowder  
Physics Department, University of California, Berkeley, CA

S.P. Ahlen  
Physics Department, Indiana University, Bloomington, IN

1. Introduction. Since the 1981 measurement by Buffington et al. [1] of a finite, low energy ( $\sim 0.1$ – $0.3$  GeV) flux of cosmic ray antiprotons ( $\bar{p}$ ), there has been a growing excitement over its possibly profound implications, since the observed flux ( $\bar{p}/p \sim 2 \times 10^{-4}$ ) is orders of magnitude larger than that predicted by standard propagation models [2]. Apart from the possibility that this single measurement is in error, numerous production models have been developed, the confirmation of any one of which would have significant or even profound astrophysical impact. These include radical modifications of propagation models [3,4],  $\bar{p}$  injection from neighboring domains of antimatter [5],  $\bar{p}$  production by evaporating primordial black holes [6,7], and most recently, cosmic ray  $\bar{p}$ 's as annihilation products of supersymmetry particles (photinos [8–10] or higgsinos [10]) that might make up the "dark" dynamical mass of the Galaxy. It is possible that  $\bar{p}$ 's originating from supersymmetric parents might have distinct spectral features that would survive solar modulation; in one model [10], higgsino annihilation proceeds through the  $b\bar{b}$  quark–antiquark channel, producing a spectral bump at  $\sim 0.3$  GeV in the  $\bar{p}$  spectrum.

2. The Detector. Because of the exciting potential signatures within the  $\bar{p}$  spectrum, we are at present designing a detector that will measure the cosmic ray  $\bar{p}$  spectrum between 0.1 and 1.0 GeV (energies at the instrument). With a payload weight of  $\sim 1000$  kg and  $\sim 100$  cm<sup>2</sup>–sr acceptance, a 2-day balloon flight over northern Canada will yield  $\sim 250$   $\bar{p}$ 's, given the Buffington et al. flux.

Unlike calorimeter detectors, our PB ( $\bar{p}$ -bar) detector identifies  $\bar{p}$ 's by directly visualizing their trajectory within a magnetic field. Figure 1 is a schematic of the PB detector. A multilayer array of high resolution drift tubes is placed within the dipole field volume of a permanent magnet. Momentum analysis of the trajectory gives particle energy and sign of charge. An aerogel Cerenkov radiator of index  $n = 1.10$  acts as a high-energy veto that eliminates much of the background, and a time-of-flight scintillator pair discriminates against albedo protons and provides a measurement of the charge magnitude.

The PB instrument makes use of advances both in drift-tube technology and in permanent magnet technology. The drift tubes to be used are based on those recently incorporated into the MAC detector at PEP, as part of a high

resolution vertex chamber [11]. They consist of 0.7 cm diameter tubes of aluminized mylar, with a wall thickness of 0.01 cm, operated at high pressure (4 atm) and high voltage (~4 kV). With a heavily quenched gas, such as 50% Ar/50% ethane, a limited streamer mode is achieved. In this mode essentially the first electron to reach the anode wire produces the entire pulse height. This has been shown to provide optimal spatial resolution [12], and reduces amplifier and cross-talk requirements as well. Measurements at SLAC found the tube resolution to be ~25  $\mu\text{m}$ . In the analysis of PB, we assume a tube resolution of 30  $\mu\text{m}$  (optimal) to 50  $\mu\text{m}$  (conservative). The drift tube array in PB will consist of ~17 layers (close-packed) of tubes with cylinder axes along the direction of the magnetic field (y-direction); these will give the projected trajectory information in the xz plane needed for curvature analysis. Two additional layer pairs with cylinder axes along the x-direction, placed above and below the main array, will provide a value for the less critical y-component of momentum.

The permanent magnet in which the drift tube array is imbedded is based on recent advances in permanent magnet materials and design. Figure 2 shows the toroidal geometry of the magnet, whose novel segmented design [13] provides a dipole field in a direction perpendicular to the opening angle of the magnet. The magnet material, neodymium-iron-boron, is a new rare-earth material with an extraordinarily high remnant field strength of ~12 kG. Computer calculations have produced a magnet design giving an interior dipole field strength of ~10 kG, with a total weight of ~225 kg. Once constructed, there are none of the failure modes that can plague a superconducting magnet system. However, as the rare earth materials are brittle, and as the mechanical forces between magnet elements are quite strong, extreme care has to be taken during its construction.

The Cerenkov radiator is a thermally sintered aerogel of refractive index  $n = 1.10$ , which will veto protons of energy  $>1.3$  GeV, and will also eliminate the  $e^-$ ,  $\mu^-$ , and  $\pi^-$  background, as those particles which do not generate a Cerenkov signal will have a measured momentum below our cutoff corresponding to a 0.1 GeV proton, as shown in Fig. 3. A total thickness of ~5 g/cm<sup>2</sup> gives ~42 photoelectrons from a muon with  $\beta = 1$  [14], of which <5% is from scintillation within the accompanying light diffusion box. Species of lower mass (except kaons) with momenta above the lower limit of 0.45 GeV/c will therefore produce signals of such high statistical significance, compared to veto threshold, that  $\bar{p}$  contamination will be negligible.

Finally, a TOF scintillator pair, separated by 50-100 cm, will screen against albedo protons, which in going backward through the detector also have the "negative" curvature which identifies the antiproton. To minimize  $\bar{p}$  energy loss and background production, the individual scintillators will be <2 cm thick, giving a TOF resolution of ~300 psec, more than adequate to detect albedo protons with  $E < 1.3$  GeV.

3. Resolution and Background. As discussed above, potential backgrounds from low-energy  $e^-$ ,  $\mu^-$ ,  $\pi^-$ 's are eliminated by the Cerenkov radiator in

concert with a low-momentum cutoff. Because of its high mass the  $K^-$  cannot be similarly screened, and in fact creates an irreducible background that must be calculated and subtracted from the  $\bar{p}$  signal. All of the  $K^-$  background is produced within our instrument upstream of the Cerenkov radiator. Using  $K^-$  multiplicity data from the CERN ISR collider [15], along with subthreshold production data from LBL's Bevalac [16], we estimate a low-energy background  $K^-/p < 10^{-5}$ . More accurate calculations are in progress.

The major factors degrading resolution and possibly contributing to background are large-angle single Coulomb scattering (SCS), multiple Coulomb scattering (MCS), and  $\delta$ -ray production. Our minimum field strength of 10 kgauss has been chosen to eliminate both SCS and MCS as a source of serious contamination. We have calculated that MCS is a minor factor in resolution degradation and is not able to generate any  $\bar{p}$  background. SCS is a more serious problem: a subthreshold proton scattered in the "negative curvature" direction must be screened with high statistical confidence. Estimated confidence levels for discriminating against a proton that has been scattered at an optimal angle for masquerading as a  $\bar{p}$ , combined with the SCS probability distribution, indicate that contamination of  $\bar{p}$ 's from this process should be negligibly small. A Monte Carlo program is now being developed to accurately determine momentum resolution as a function of energy when MCS, SCS and  $\delta$ -ray production are fully taken into account.

### References

1. A. Buffington, S.M. Schindler and C.R. Pennypacker, *Ap. J.* 248, 1179 (1981).
2. T.K. Gaisser and R.H. Mauger, *Phys. Rev. Lett.* 30, 1264 (1973); T.K. Gaisser and B.G. Maurer, *Ap. J.* 252, L57 (1982).
3. L.C. Tan and N.K. Ng, *Ap. J.* 269, 751 (1983); L.C. Tan and N.K. Ng, *Proc. 18th Inter. Cosmic Ray Conf.*, (Bangalore) 2, 90 (1983).
4. S.A. Stephens and B.G. Mauger, to be published in *Astrophys. Sp. Sci.*
5. F.W. Stecker, *Nucl. Phys. B* (1984), and references there in.
6. P. Kiraly, J. Szabelski, J. Wdowczyk and A.W. Wolfendale, *Nature* 293, 120 (1981).
7. M.S. Turner, *Nature* 297, 379 (1982).
8. J. Silk and M. Srednicki, *Phys. Rev. Lett.* 53, 624 (1984).
9. F. Steck, personal communication.
10. J.S. Hagelin and G.L. Kane, to be published.
11. E. Fernandez et al., SLAC PUB 3390, August, 1984.
12. J. Va'vra, SLAC-PUB 3131, June, 1983.
13. K. Halbach, LBL Report No. 8906, March, 1979.
14. S.M. Schindler, personal communication.
15. A. Antinucci et al., *Lett. Nuovo Cim.* 6, 121 (1973).
16. A. Shor et al., *Phys. Rev. Lett.* 48, 1597 (1982).

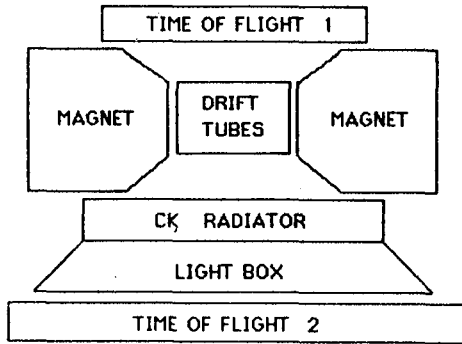


Fig. 1. Schematic showing detector elements of PB (not to scale).

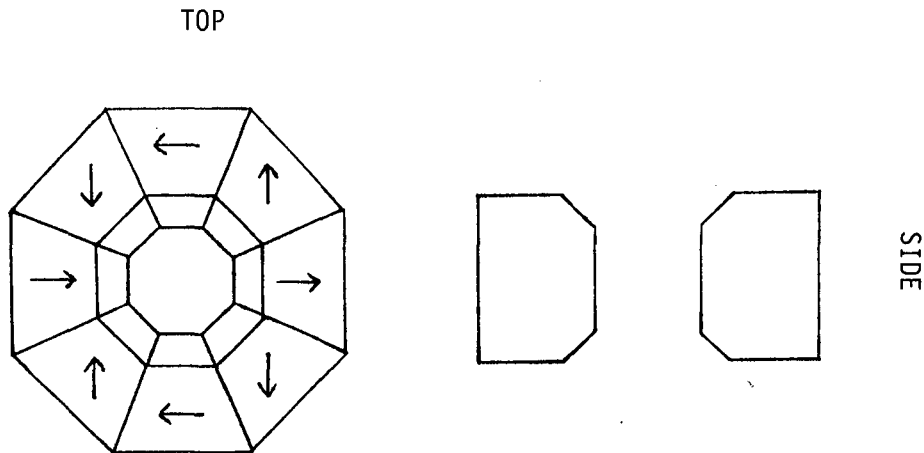


Fig. 2. Permanent magnet geometry (not to scale). Arrows within each segment show magnetization direction, with the summed field giving a dipole field in the central volume.

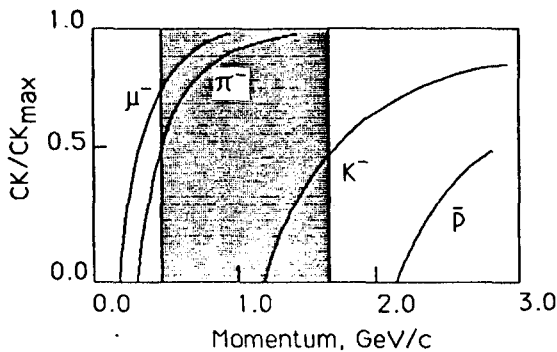


Fig. 3. Cerenkov emission from radiator as a function of particle species and momentum. Events are accepted only within the shaded interval.